Embedded Photonic Eigenvalues in 3D Nanostructures

Francesco Monticone and Andrea Alù*
Department of Electrical and Computer Engineering, The University of Texas at Austin, Austin, Texas 78712, USA
(Received 9 March 2014; published 29 May 2014)

Confinement of light is usually achieved by reducing the photonic density of states of the surrounding environment, as in waveguides and photonic crystal cavities. In contrast, optical bound states have been recently shown to exist within the radiation continuum in large periodic arrays, in analogy with embedded eigenvalues in certain quantum systems. Here we demonstrate that under special conditions it may be possible to induce three-dimensional photonic embedded eigenvalues in a subwavelength open scattering system. The striking properties of these optical states without radiation loss may lead to unprecedented light localization in nanophotonic structures.

DOI: 10.1103/PhysRevLett.112.213903 PACS numbers: 42.25.Bs, 73.20.Mf, 78.67.Pt

Following the discovery of the wave properties of light and matter in the last two centuries, the ability to localize and confine waves has become of extreme importance in modern science. It is well known that an optical state coupled to radiation modes gradually loses its energy in the background. Light confinement, or the creation of a bound state, is conventionally achieved by suppressing these radiation channels, e.g., by surrounding a region of space with reflectors, or with photonic band-gap materials [1]. These solutions typically require volumes comparable or larger than the diffraction limit and may pose challenges in their efficient excitation with an external source. More recently, large light confinement has been achieved in plasmonic nanostructures supporting subradiant, or dark, optical states. When coupled to a bright dipolar mode, these states can be efficiently excited, producing Fano interference effects [2] and strongly localized fields, exhibiting lower radiation damping than conventional plasmonic resonances [3]. However, light confinement is still modest in these structures due to the residual radiation loss associated with the dark mode.

It has recently been shown, quite surprisingly, that it is in principle possible to ideally confine a bright optical mode within the radiation continuum, realizing an ideal optical bound state surrounded by symmetry-compatible radiation modes. The idea stems from the discovery in quantum mechanics that certain quantum systems can support spatially localized electrons with energy larger than their potential barriers [4,5]. These bound states within the continuum, indicated as embedded eigenvalues (EEs), are generally understood as the result of an interference mechanism that produces a resonance with infinite lifetime [6–8]. Recently, these concepts have been extended to electromagnetic waves, leading to the theoretical [9] and experimental [8] demonstrations of optical bound states within the light cone. These optical EEs are not based on symmetry incompatibility, as in [10], but rather on destructive interference, analogous to their quantum counterparts. So far, however, all of these proposals have been limited to two-dimensional (2D) infinite geometries, such as unbounded photonic crystal slabs [8,9]. In this Letter, we show that analogous EEs can also be supported by open three-dimensional (3D) subwavelength nanostructures, realizing an ideally confined optical state, even in the presence of available and symmetry-compatible radiation channels.

We start by considering the classical problem of electromagnetic wave interaction with a layered nanosphere, as in the inset of Fig. 1. In the exact Mie solution of Maxwell's equations [11], the scattering coefficient of the nth spherical harmonic can be written as $c_n = -U_n/(U_n + iV_n)$ [12], where the quantities U_n and V_n are expressed as a combination of spherical Bessel and Neumann functions under an $e^{-i\omega t}$ time dependence. When $U_n = 0$, the scattering coefficient vanishes, corresponding to a "scattering zero." Conversely, $V_n = 0$ yields a "scattering resonance," as the coefficient is unitary and the maximum energy is coupled into the associated radiation channel. If the entire denominator vanishes, $U_n + iV_n = 0$, and U_n is nonzero, the scattering coefficient goes to infinity, corresponding to a "scattering pole." Such singularities in the scattering response correspond to the natural modes of oscillation, or eigenmodes, of the open spherical cavity, and the associated eigenfrequencies are generally complex: $f = f_r + i f_i$. The imaginary part f_i, negative due to passivity and causality, represents the eigenmode oscillation damping and, in the lossless case, is directly related to the energy leakage in the corresponding radiation channel (radiation loss). When the sphere is small compared to the wavelength, radiation (or scattering) is dominated by the electric dipole contribution, corresponding to the $n = 1$ transverse-magnetic (TM) harmonic. The dynamic electric polarizability of the object $\alpha_d = -i6\pi c_1^{TM}\varepsilon_0/k_0^3$, with ε_0 being the free-space permittivity and k_0 the corresponding wave number, is a measure of the overall scattering properties in this limit, and its inverse is compactly written as

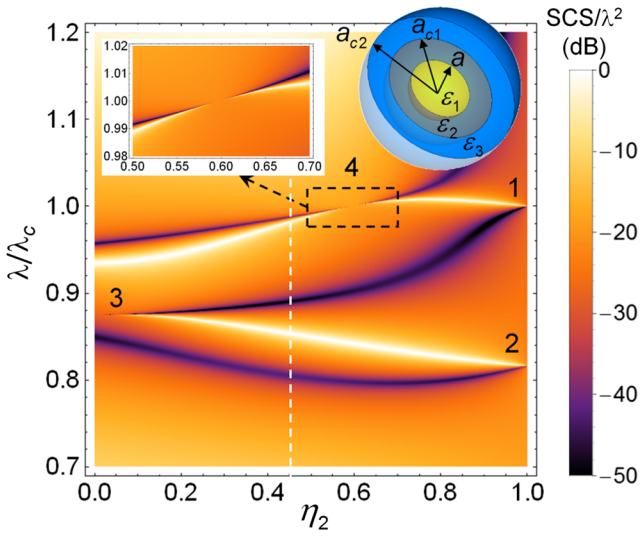

FIG. 1 (color online). Normalized scattering cross section (SCS) of the layered particle in the right inset, as a function of the aspect ratio $\eta_2 = a/a_{c2}$ and wavelength ($\lambda_c = 378$ nm). The characteristics of the composite sphere are described in the text. Numbers within the contour plot indicate the regions where Fano features disappear, as their lifetime diverges (a detail of region 4 is shown in the left inset). The vertical dashed line indicates the geometry considered in Fig. 2.

$$\alpha_d^{-1} = \frac{V_1^{TM}}{U_1^{TM}} \frac{k_0^3}{6\pi\varepsilon_0} - i\frac{k_0^3}{6\pi\varepsilon_0}. \quad (1)$$

Since V_1^{TM} and U_1^{TM} are purely real in the lossless case, $\mathrm{Im}[\alpha_d^{-1}]$ does not depend on the properties of a lossless object, but only on the environment, as it corresponds to the imaginary part of the electromagnetic Green's function at the sphere location, representing the local photonic density of states (DOS). A straightforward way to modify its value is to change the surrounding environment, in order to enhance or suppress the radiation or scattering from the object [13]. For example, inside a photonic-crystal cavity the photonic DOS is minimal, which may be exploited to prevent scattering or emission and realize a bound state [1]. In this situation, the inverse polarizability (1) is purely real, and the structure supports real eigenfrequencies (solutions of $\alpha_d^{-1} = 0$), corresponding to ideal scattering poles with infinite lifetime that realize a bound optical state. Our goal here, on the contrary, is to show that it is possible to obtain a bound optical state by properly tailoring the geometry of the object without changing the photonic DOS of the surrounding environment, thereby realizing an EE within the continuum of radiation modes. A relevant result in this context has been recently presented [14] while analyzing the scattering features of a dielectric sphere supporting a magnetic resonance when surrounded by an ideal zero-permittivity shell, which was shown to correspond to an unlimited Q factor in this ideal limit. Here, we explore the general conditions to achieve real-valued scattering eigenfrequencies in 3D subwavelength nanoparticles and unveil the fundamental relations to the physics of EEs.

The scattering eigenfrequencies in free space are generally not real, but they tend to get closer to the real axis for small lossless objects because radiation is less and less efficient as their electrical size shrinks. In this regime, scattering dips and resonances necessarily alternate along the real frequency axis, analogous to Foster's reactance theorem for passive circuit elements [15,16]. This feature was exploited in [17,18] to realize sharp scattering features based on closely spaced scattering zeros and poles supported by composite subwavelength nanoparticles. These findings indicate that specific nanoparticle geometries may be able to largely tailor the eigenmodal scattering properties, even though the local DOS is left unchanged.

To demonstrate that this is the right path toward the synthesis of 3D EEs, let us go back to the layered sphere example of Fig. 1. We assume that the particle is composed of a dielectric core with relative permittivity $\varepsilon_1 = 1.5$ and radius a, surrounded by two plasmonic shells of radius a_{c1} and a_{c2}, respectively, and characterized by lossless silverlike Drude models, $\varepsilon_{2,3} = 5 - \omega_{p2,3}^2/\omega^2$, with slightly different plasma frequencies ω_p. Here, we consider a fixed outer radius $a_{c2} = 50$ nm, while the other dimensions are determined by the aspect ratios $\eta_1 = a_{c1}/a_{c2}$ and $\eta_2 = a/a_{c2}$. For the following example, we assume that $\omega_{p2} = 2\pi 2175$ THz (silver), $\omega_{p3} = 2\pi 1775$ THz, and that the two plasmonic layers have the same thickness, such that a single aspect ratio determines the whole structure. Under these assumptions, we plot in Fig. 1 the total scattering cross section of the particle, computed with the exact Mie theory [11], as a function of η_2 and wavelength. Since the composite nanoparticle is electrically small ($k_0 a_{c2} \ll 2\pi$), the dark and bright regions of this contour plot correspond, respectively, to the scattering zeros and resonances of the dominant electric dipole harmonic. Because of Foster's theorem for scattering discussed above, the different branches cannot cross. However, when scattering zeros and resonances get close along the frequency axis, they determine dipole-dipole Fano interference features in the scattering spectrum, generally due to the interplay of surface plasmons residing on the different spherical interfaces [17,18]. In a few regions of this contour plot, we can observe Fano resonances becoming sharper and sharper and eventually disappear when their quality factor goes to infinity. This is especially evident in the dashed box and corresponding inset in Fig. 1, where the bright and dark branches appear to touch each other, producing an infinitely fine Fano feature, which eventually disappears at the tangent point. This feature is a direct indication that the resonance lifetime diverges so that it cannot any longer couple with free-space excitation, a clear signature of the presence of an embedded bound scattering state with zero radiation damping, consistent with the observations of EEs in 2D photonic crystal slabs [8].

It is evident that Fano resonances with an unbounded lifetime can be achieved in this open 3D system at the degeneracy of a scattering zero and a scattering resonance, namely for $U_1^{TM} = V_1^{TM} = 0$. The nontrivial solutions of this nonlinear system of equations can be found in the quasistatic regime as (i) $\eta_2 \to 1$ and $\varepsilon_2 \to 0$ (or $\varepsilon_3 \to 0$), related to the Fano resonances for thin shells studied in [18] (points 1 and 2 in Fig. 1); (ii) $\eta_2 \to \eta_1$ and $\varepsilon_2 \to 0$, i.e., when the first shell has a vanishing thickness and zero permittivity (case not considered in Fig. 1); (iii) $\eta_2 \to 0$ and $\varepsilon_2 = -\varepsilon_1/2$, which corresponds to a Fano resonance in the first shell, appearing when the dielectric core is very small (point 3); and (iv) finally, another resonance with a diverging lifetime that occurs when (point 4)

$$\frac{\eta_2^3}{\eta_1^3} = \frac{2\varepsilon_2 + \varepsilon_1}{2(\varepsilon_2 - \varepsilon_1)} \quad \text{and} \quad \varepsilon_3 \to 0. \tag{2}$$

Each of these conditions requires some extreme feature in the nanoparticle, which is not surprising as we are analyzing the mathematical limit in which the resonance lifetime goes ideally to infinity. Interestingly, three of these conditions require one of the concentric layers to have a permittivity identically equal to zero, consistent with the recent theoretical findings in [14], but in general based on different underlying phenomena. In particular, the last condition [Eq. (2)] extends the results in [14] to the subwavelength limit, as it synthesizes in the inner core-shell particle a subdiffractive quasistatic magnetic resonance enclosed by a zero-permittivity outer shell. Conditions (i) and (ii), instead, are related to the excitation of volume plasmons in zero-permittivity shells with vanishing thickness and are independent of the core and surrounding material, as we further discuss in [19]. Finally, condition (iii) highlights yet a different mechanism leading to an EE, for which infinite lifetime is achieved at the inner interface with a vanishingly small radius, and in contrast with the findings in [14], it proves that zero-permittivity materials may not be generally required to achieve this phenomenon [19]. In general, these results demonstrate that it is indeed possible to achieve infinite lifetimes in subwavelength open nanoparticles.

In order to elucidate the generation and dynamics of these anomalous embedded scattering eigenstates, we focus on the case in Eq. (2) as an example, but similar considerations apply also to the other conditions derived above, which are further explored and discussed in [19]. In the example of Fig. 1, the requirements for the EE are met when $\eta_2 = \eta_{2,ee} = 0.597$ and $\lambda = \lambda_c = 378$ nm [calculated with full-dynamic Mie theory, yielding slightly different values than with the quasistatic Eq. (2)]. It is now useful to visualize the position of the eigenfrequencies in the complex plane as we approach this condition. Consider first a slightly different aspect ratio $\eta_2 = 0.45$ (vertical dashed line in Fig. 1). Self-sustained oscillations (eigenmodes) are obtained

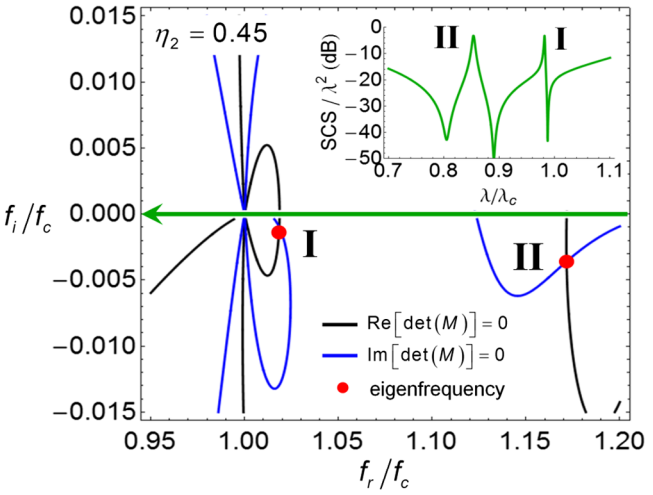

FIG. 2 (color online). Eigenfrequencies (red dots) on the complex frequency plane, for the layered sphere in Fig. 1, with aspect ratio $\eta_2 = 0.45$ (vertical dashed line in Fig. 1). The central frequency is $f_c = (3 \times 10^8 \text{ m/s})/\lambda_c = 794$ THz. Black (blue) lines indicate where the real (imaginary) part of the determinant of the boundary condition matrix M goes to zero. The inset shows the normalized SCS of the composite sphere on the real wavelength axis (thick green arrow).

when the coefficient matrix M of the linear system formed by the electromagnetic boundary conditions becomes singular. We plot in Fig. 2 the dispersion of the conditions $\text{Re}[\det(M)] = 0$ (black line) and $\text{Im}[\det(M)] = 0$ (blue), in the complex frequency plane, for the TM_1 spherical harmonic. When the curves intersect (red circles), the matrix is singular, which corresponds to a scattering eigenmode. Two eigenfrequencies are visible in the frequency range considered in Fig. 1, indicated by points I and II in Fig. 2. When the particle is illuminated, the impinging wave produces the resonant features visible in the scattering spectrum shown in the inset of Fig. 2. Eigenmode I is the one of interest since it induces a sharp Fano resonance with small, yet finite, radiation damping. As we increase the ratio η_2, the eigenfrequency I moves closer and closer to the real frequency axis, as shown in Fig. 3(a), until it becomes purely real when condition (2) is identically met. At the same time, we also see that the lifetime of the associated Fano resonance in the scattering spectrum diverges [insets of Fig. 3(a)]. This analysis confirms the realization of an EE within the radiation continuum, corresponding to an eigenmode of the spherical particle embedded along the real frequency axis. Remarkably, such an ideally confined optical state, based on purely dipolar fields, exists despite the presence of symmetry-compatible radiation channels (the photonic DOS of the surrounding medium has not been altered, and dipolar radiation is obviously allowed). It is indeed rather striking that the realized EE is of purely dipolar order, a harmonic that tends to strongly couple to free-space radiation.

Further physical insights can be gained by analyzing the field distribution of the embedded eigenmode. As we

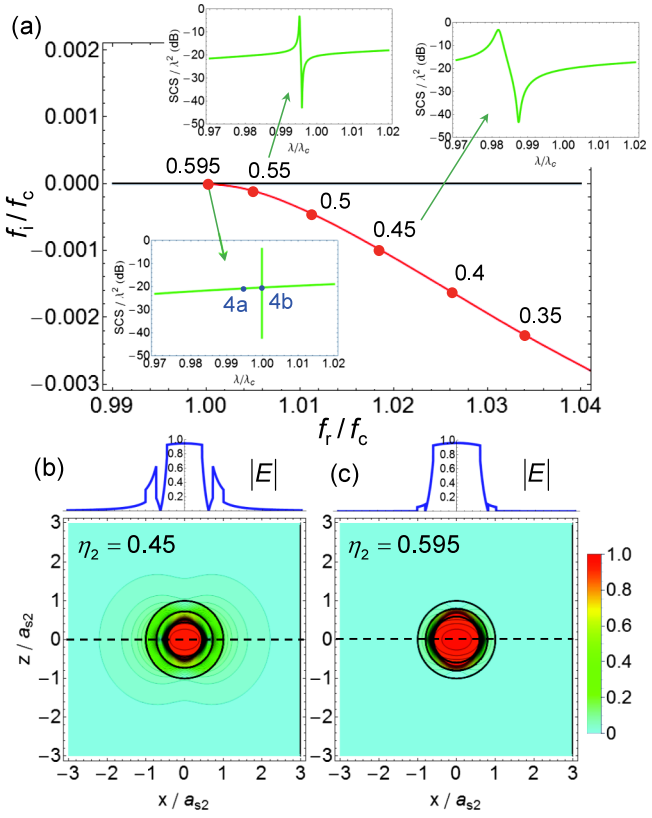

FIG. 3 (color online). (a) Evolution of the eigenfrequency I of Fig. 2 on the complex frequency plane, as the particle aspect ratio (numbers accompanying the red dots) approaches $\eta_{2,ee} = 0.597$. The insets show the normalized SCS of the composite sphere for different aspect ratios. The blue dots and labels in the bottom left inset indicate the frequencies considered in Fig. 4. (b) and (c) Electric field intensity of the eigenmode for $\eta_2 = 0.45$ (b) and $\eta_2 = 0.595$ (c). On top of (b) and (c), we also show the electric field intensity along the x axis (black dashed lines).

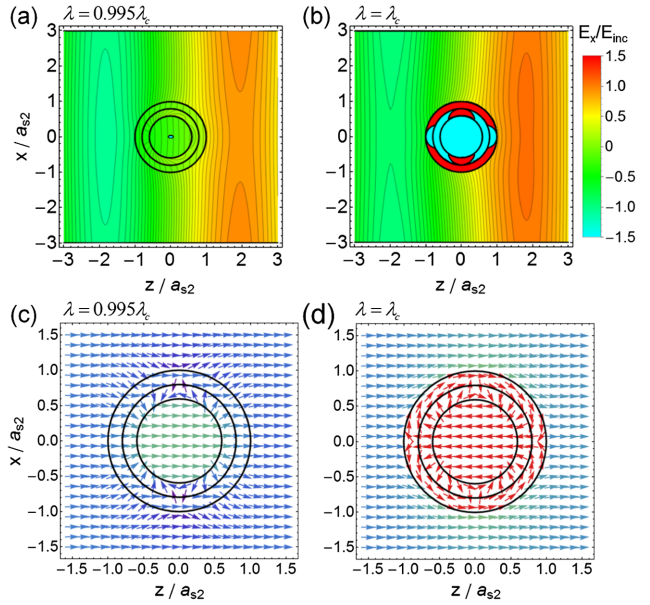

FIG. 4 (color online). (a) and (b) Electric field distribution (time snapshot of the x component) on the E plane, for the layered nanosphere with aspect ratio $\eta_2 = 0.595$, illuminated by a plane wave of wavelength $\lambda = 0.995\lambda_c$ (a) and $\lambda = \lambda_c$ (b) [blue dots in the bottom left inset of Fig. 3(a)]. (c) and (d) Time-average Poynting vector distribution at $\lambda = 0.995\lambda_c$ (c) and $\lambda = \lambda_c$ (d). The same color scale is used in (c) and (d), with warmer colors corresponding to higher intensity. In all panels, the impinging plane wave propagates from left to right.

increase the aspect ratio from $\eta_2 = 0.45$ [Fig. 3(b)] to $\eta_2 = 0.595$ [Fig. 3(c)], the latter being very close to $\eta_{2,ee}$, we clearly see that the field distribution of the eigenmode becomes more localized inside the particle, while the external field tends to vanish. Indeed, the embedded eigenmode is characterized by zero fields outside the composite sphere, as clearly seen in Fig. 3(c). It should be noted that this property holds for all resonances with infinite lifetime identified in Fig. 1, including the one that does not require epsilon-near-zero layers (point 3 in Fig. 1). This property highlights a significant difference between EEs in 2D and 3D geometries: while in the 2D case [8,9] the bound state is characterized by evanescent fields outside the structure, analogous to a surface mode, in this 3D open scenario EEs with finite fields in the external region are not available, as spherical harmonics are always radiative [20]. While in Figs. 3(b) and 3(c) we plotted the self-sustained eigenmodal field distributions assuming no excitation, we consider now the optical response of the particle under external plane-wave excitation. As seen in the bottom left inset of Fig. 3(a) ($\eta_2 = 0.595$), when the eigenfrequency is extremely close to the real frequency axis, the EE appears in the scattering spectrum as a very narrow spike emerging from a smooth dipolar background radiation. For this case, in Figs. 4(a) and 4(b), respectively, we plot time snapshots of the electric field distribution at a frequency slightly off-resonance, $\lambda = 0.995\lambda_c$, and at the center of the ultranarrow Fano resonance, $\lambda = \lambda_c$ [blue dots in the inset of Fig. 3(a)]. Interestingly, the field outside the particle is very similar in the two cases, as it corresponds to the same dipolar radiation background. However, the internal fields are drastically different, and notably, the optical response at $\lambda = \lambda_c$ [Fig. 4(b)] exhibits an extremely large field intensity, despite the weak external scattering, essentially identical to the eigenmodal distribution. As shown in [19], the stored energy in the core indeed diverges as the aspect ratio approaches $\eta_{2,ee}$. The corresponding time-average Poynting vector distributions in Figs. 4(c) and 4(d) highlight even more strikingly this peculiar behavior. At frequencies slightly off resonance [Fig. 4(c)], the impinging power (from left to right) simply flows through the particle as one would expect in a weakly scattering nanostructure; conversely, at the frequency of the EE [Fig. 4(d)], a large amount of energy is trapped in a self-sustained power flow within the open cavity, supporting an embedded eigenmode very weakly coupled to outside radiation. This residual coupling would

completely disappear at the exact condition $U_1^{TM} = V_1^{TM} = 0$, for which an infinitely long lifetime is achieved, and the eigenmode would not be excited at all by the external plane wave (but it would by a source placed inside the nanoparticle). In conclusion, we have theoretically demonstrated the general conditions to realize purely dipolar EEs supported by subwavelength lossless 3D structures. The described optical bound states exhibit unprecedented localization of light in a subwavelength volume, despite the presence of symmetry-compatible radiation modes in the background. The derived conditions for ideal light confinement and infinite stored energy all imply extreme values of geometry or material parameters, which is consistent with the requirement of an ideally infinite structure to support EEs in 2D configurations [8]. Small detuning from these ideal conditions restores finite, yet in principle as large as desired, stored energy and oscillation lifetime [19]. Although the requirement of small absorption may be challenging to achieve, gain media may be exploited to compensate natural Ohmic losses of plasmonic materials, providing a route to take full advantage of the striking properties of these EEs. The extreme localization and enhancement of light may find application in several diverse practical scenarios, from enhanced nonlinear phenomena to sensing, as well as thermal ablation of tumors and nanolasing.

This work was supported by the AFOSR with Grant No. FA9550-13-1-0204, the Welch Foundation and the ONR with Grant No. N00014-10-1-0942.

*alu@mail.utexas.edu

[1] E. Yablonovitch, Phys. Rev. Lett. **58**, 2059 (1987).
[2] B. Luk'yanchuk, N. I. Zheludev, S. A. Maier, N. J. Halas, P. Nordlander, H. Giessen, and C. T. Chong, Nat. Mater. **9**, 707 (2010).
[3] M. I. Stockman, Nature (London) **467**, 541 (2010).
[4] J. von Neuman and E. Wigner, Phys. Z. **30**, 465 (1929).
[5] F. Capasso, C. Sirtori, J. Faist, D. L. Sivco, S.-N. G. Chu, and A. Y. Cho, Nature (London) **358**, 565 (1992).
[6] F. H. Stillinger and D. R. Herrick, Phys. Rev. A **11**, 446 (1975).
[7] H. Friedrich and D. Wintgen, Phys. Rev. A **32**, 3231 (1985).
[8] C. W. Hsu, B. Zhen, J. Lee, S.-L. Chua, S. G. Johnson, J. D. Joannopoulos, and M. Soljačić, Nature (London) **499**, 188 (2013).
[9] D. C. Marinica, A. G. Borisov, and S. V. Shabanov, Phys. Rev. Lett. **100**, 183902 (2008).
[10] Y. Plotnik, O. Peleg, F. Dreisow, M. Heinrich, S. Nolte, A. Szameit, and M. Segev, Phys. Rev. Lett. **107**, 183901 (2011).
[11] C. F. Bohren and D. R. Huffman, *Absorption and Scattering of Light by Small Particles* (John Wiley & Sons, New York, 2008).
[12] A. Alú and N. Engheta, J. Appl. Phys. **97**, 094310 (2005).
[13] E. M. Purcell, Phys. Rev. **69**, 681 (1946).
[14] M. G. Silveirinha, Phys. Rev. A **89**, 023813 (2014).
[15] N. Engheta, A. Salandrino, and A. Alú, Phys. Rev. Lett. **95**, 095504 (2005).
[16] R. M. Foster, Bell Syst. Tech. J. **3**, 259 (1924).
[17] F. Monticone, C. Argyropoulos, and A. Alú, Sci. Rep. **2**, 912 (2012).
[18] F. Monticone, C. Argyropoulos, and A. Alú, Phys. Rev. Lett. **110**, 113901 (2013).
[19] See Supplemental Material at http://link.aps.org/supplemental/10.1103/PhysRevLett.112.213903 for an analysis of the stored and radiated energies under plane-wave illumination, the effect of Ohmic losses and a thorough discussion on the different conditions leading to 3D EEs and their underlying mechanism.
[20] D. Colton and R. Kress, *Inverse Acoustic and Electromagnetic Scattering Theory* (Springer, Berlin, 1998).